Study of Two Novel Permanent-Magnet Vernier Machines with Quantitative Comparison and Experimental Verifications

Jiangui Li, K.T. Chau and J.Z. Jiang
Department of Electrical and Electronic Engineering
The University of Hong Kong, Hong Kong
jgli@eee.hku.hk

Abstract—In this paper, a new permanent-magnet vernier (PMV) machine has been proposed and the performances have been analyzed based on the comparison with its counterpart, namely, the magnetic-geared machine. An analytical approach to calculate the airgap flux distribution and the torque in proposed PMV machine has been presented. Then the finite element method is used to analyze the harmonic order of the key factors. The analytical analysis results agree well with those obtained by the finite element analysis and experimental results. Finally, the proposed machine has been prototyped for experimentation.

I. INTRODUCTION

Vernier machine as one member of harmonic machine family has been known as a promising candidate for low-speed high-torque applications [1]-[3]. The highly nonlinear relationship between the dimensions and magnetic field makes the design cumbersome. At present, only the fundamental component is considered for maximizing the output torque [4], [5]. However, the harmonics corresponding to the winding pole-pair, flux-modulation pole-pair and the rotor pole-pair in the airgap flux density are non-neglectable. In this paper, we present an analytical approach to calculate the airgap flux distribution, the magnetic motive force and the torque in proposed permanent-magnet vernier (PMV) machine, as shown in Fig. 1 (a), called as Machine I in this paper. And the other machine coined as magnetic-geared machine has be shown in Fig. 1 (b), called as Machine II in this paper.

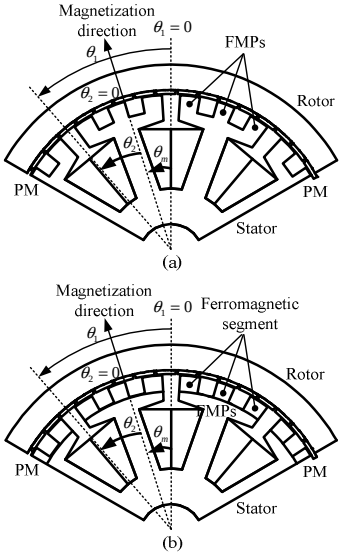

Fig. 1. Machine Topologies. (a) Machine I. (b) Machine II.

II. THEORETICAL ANALYSIS

The knowledge of the field distribution in the airgap of the PMV is vitally important for predicting and optimizing its performance [6]. A group of analytical equations concerning the airgap flux density and the torque are evaluated considering the harmonics to describe the behavior of the proposed machine shown by (1) and (2), and the results will be given in the full paper because of the limited space. The definitions of mechanical angles are shown in Fig. 1.

$$B \approx B_{PMh}\cos\left[Z_2\left(\theta_1-\theta_m\right)\right]+\frac{1}{2}B_{PM1}\cos\left[\left(Z_2-Z_1\right)\theta_1-Z_2\theta_m\right] \quad (1)$$

$$T=\frac{p\lambda l}{\pi}\int_0^{2\pi}\left[P\left(F_c+F_{PM}\right)\right]\frac{\partial F_{PM}}{\partial\theta_m}d\theta_1 \quad (2)$$

III. SIMULATION RESULTS AND EXPERIMENTAL VERIFICATION

The flux distributions of both machines at 0° and 90°are shown in Fig. 2. It can be observed that the flux lines per stator tooth can pass through the FMPs separately, hence verifying the desired flux modulation. It also can be seen that the flux line changes a lot when the rotor rotates one fourth of the pole pitch. The airgap flux density and its harmonic spectra of Machine I, inner airgap of Machine II and outer airgap of Machine II are given in Fig. 3, Fig. 4 and Fig. 5, respectively. It has shown that, the airgap flux density of the outer airgap of Machine II has the same number of poles with Machine I while has smaller value owing to two airgaps introduced by the ferromagnetic segments. Then, the torque transmission characteristic is obtained through calculating the locked-rotor operation.

The corresponding no-load EMF and the output torque waveforms obtained by the finite element method are described in Fig. 6. The amplitudes of no-load EMF of Machine I and Machine II are 98 V and 75.2 V, while the output torques are 69.1 Nm and 55.2 Nm. Namely, the torque-handling capability is 30.3% and the no-load EMF is 25% of the proposed machine Machine I higher than the Machine II. It also can be seen that the no-load EMF waveform is almost perfectly sinusoidal, which is desirable for smooth torque production.

The measured waveforms of no-load EMF and no-load EMF vs. versus speed are shown in Fig. 7. It has been seen that the torque of Machine II has slight phase shift compared to Machine I. The analytical analysis results, namely, the field distribution, no-load EMF and the torque transmission performance agree well with those obtained by the finite element method and experimental results. The detailed simulation and experimental results will be given in the full

paper.

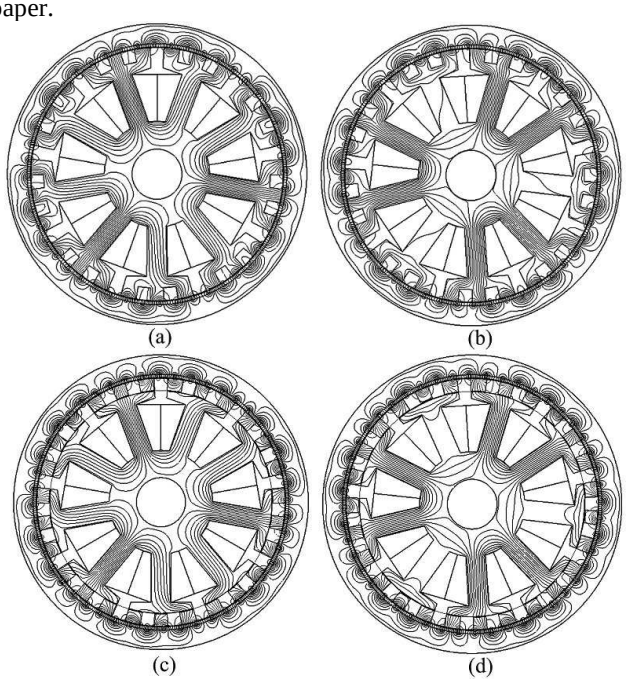

Fig. 2. Flux distribution. (a) Machine I at 0°. (b) Machine I at 90°. (c) Machine II at 0°. (d) Machine II at 90°.

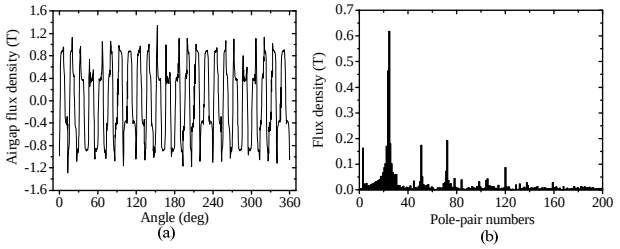

Fig. 3. Airgap flux density of Machine I. (a) Waveform. (b) Harmonic spectra.

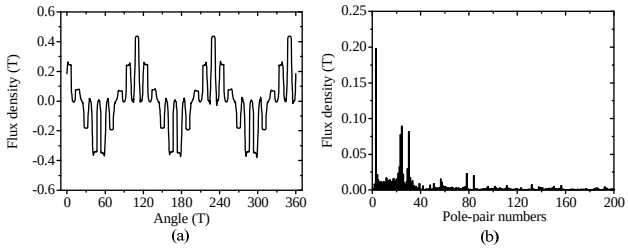

Fig. 4. Inner airgap flux density of Machine II. (a) Waveform. (b) Harmonic spectra.

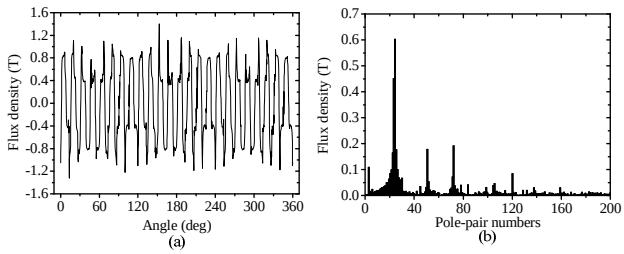

Fig. 5. Outer airgap flux density of Machine II. (a) Waveform. (b) Harmonic spectra.

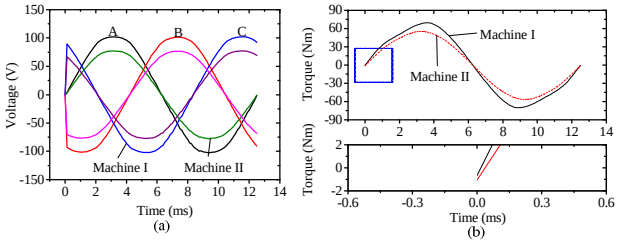

Fig. 6. Simulated no-load EMF and torque. (a) Waveform. (b) Harmonic spectra.

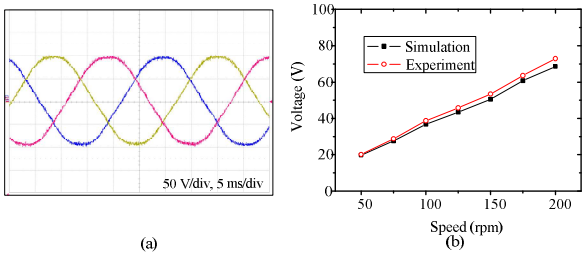

Fig. 7. Measured no-load EMF. (a) Waveform measured at 200 rpm. (b) No-load EMF vs. speed.

IV. Conclusion

Vernier machine has been known as a promising candidate for low-speed high-torque applications. A new PMV machine has been proposed and the performances of has been analyzed based on the comparison with so-called magnetic-geared machine. The key parameters, namely the airgap flux distribution, no-load EMF and the torque in proposed PMV machine have been analyzed by an analytical approach, finite element method and then verified by the experiment. The analytical analysis results agree well with those obtained by the finite element method and experimental results. It has also shows that the newly proposed machine has a large improvement compared to its counterpart.

V. References

[1] A. Toba, and T. A. Lipo, "Generic torque-maximizing design methodology of surface permanent-magnet vernier machine," *IEEE Trans. on Industry Appl.*, vol. 36, no. 6, 2000, pp. 1539-1546.

[2] E. Spooner and L. Haydock, "Vernier hybrid machines," *IEE Proc. of Elec. Power Appl.*, vol. 150, no. 6, 2003, pp. 655-662.

[3] J. G. Li, K. T. Chau, J. Z. Jiang, C. H. Liu and W. L. Li, "A new efficient permanent-magnet vernier machine for wind power generation," *IEEE Trans. on Magn.*, vol. 45, no. 6, 2010, pp. 1475-1478.

[4] L. N. Jian, and K. T. Chau, "A magnetic-geared outer-rotor permanent-magnet brushless machine for wind power generation," *IEEE Trans. on Industry Appl.*, vol. 45, no. 3, 2009, pp. 954-962.

[5] K. T. Chau, D. Zhang, J. Z. Jiang, C. H. Liu, and Y. J. Zhang, "Design of a magnetic-geared outer-rotor permanent-magnet brushless motor for electric vehicles," *IEEE Trans. on Magn.*, vol. 43, no. 6, 2007, pp. 2504-2506.

[6] Z. Q. Zhu and D. Howe, "Instantaneous magnetic field distribution in brushless permanent magnet dc motors, Part III: Effect of stator slotting," *IEEE Trans. on Magn.*, vol. 29, no. 1, 1993, pp. 143-151.